

N68-19192

**NASA CONTRACTOR
REPORT**



NASA CR-1043

NASA CR-1043

**SUBSOLAR-MERIDIAN MEAN-ANNUAL
DISTRIBUTIONS FOR MARTIAN
TROPOSPHERE BELOW 50 KILOMETERS**

by F. C. Bates

Prepared by
SAINT LOUIS UNIVERSITY
Saint Louis, Mo.
for Langley Research Center

SUBSOLAR-MERIDIAN MEAN-ANNUAL DISTRIBUTIONS FOR
MARTIAN TROPOSPHERE BELOW 50 KILOMETERS

By F. C. Bates

Distribution of this report is provided in the interest of information exchange. Responsibility for the contents resides in the author or organization that prepared it.

Prepared under Grant No. NGR-26-006-016 by
SAINT LOUIS UNIVERSITY
Saint Louis, Mo.

for Langley Research Center

NATIONAL AERONAUTICS AND SPACE ADMINISTRATION

For sale by the Clearinghouse for Federal Scientific and Technical Information
Springfield, Virginia 22151 - CFSTI price \$3.00

Abstract

Available observations of the Martian atmosphere, including those of Mariner IV, spectrometric and photographic observations, were employed to estimate the composition of the homogeneous atmosphere and equivalent-mean-sea-level pressure. A mean-annual subsolar-meridian distribution of temperature, pressure and zonal-wind speed was then constructed for a depth of 50 km. based on the foregoing estimates and: (1) an assumed -- and subsequently verified for consistency -- wave regime; (2) hydrostatic balance; (3) midlatitude scale height consistent with Mariner IV observation; (4) tropopause height varying from 30 km. at the equator to 10 km. at the pole; (5) mean jet-stream position at 45° latitude and 20 km.; and (6) estimates from similarity to Earth and other rotating-fluid systems.

These results were then extended to an estimate of wind and wind regimes, including secondary circulations such as extra-tropical cyclones and yellow-dust devils. Computations of heating rates in a ten-layer model derived by A. J. Pallmann were used to test soundings at several latitudes to determine required dynamic and/or advective compensation.

TABLE OF CONTENTS

Background.....	1
Composition.....	1
Mean-Annual Subsolar-Meridian	
Surface-Temperature Distribution.....	3
Depth of Troposphere.....	5
Lapse Rates of Temperature.....	5
Mode of General Circulation.....	6
Surface Pressure Distribution.....	7
Aspects of the Equatorial Sounding.....	8
Water Vapor in Mixed Columns.....	12
Aspects of the Mid-Latitude Sounding.....	14
Aspects of the Polar Sounding.....	14
Some Circulation Estimates.....	14
Mean-Annual Subsolar-Meridian	
Cross-Section.....	15
Storm and Local Circulations.....	15
Surface-Wind-Speed Probabilities in	
Random Entries.....	18
Estimates of Lateral (Meridional) and	
Vertical Speeds.....	18
Radiation Checks on Estimated Soundings.....	22
Deduction of Circulation from	
Planetary Markings.....	25
Current Estimates of Atmospheric Magnitudes.....	27
Conclusions and Further Research.....	29

TABLE OF CONTENTS cont'd.

Acknowledgments..... 31
References..... 32
Appendix..... 34

List of Illustrations

	Page No.
Figure 1. Interpretation of the immersion portion of the Mariner IV occultation. Heavy solid line is suggested temperature curve. Cutoff on elevated point is illustrated. Base diagram is T-lnP type for 100% CO ₂ atmosphere.	2
Figure 2. Estimated equator-pole distribution of mean-annual subsolar-meridian surface temperature for Mars.	4
Figure 3. Equatorial mean-annual subsolar-meridian sounding for Mars.	9
Figure 4. Mid-latitude (45° lat.) mean-annual subsolar meridian sounding for Mars.	10
Figure 5. Polar mean-annual sounding for Mars.	11
Figure 6. Mean-annual subsolar-meridian cross-section for Mars. Hemispheric symmetry is assumed in the first approximation.	13
Figure 7. Dewpoint-temperature ranges for various depths of mixed columns corresponding to a range of contained water (precipitated depth) from 7 to 21 microns.	16
Figure 8. Estimated probability distribution of surface (gradient wind level) wind speeds in a random entry into the Martian atmosphere.	19
Figure 9. Several suggested temperature distributions used in heating-rate computations.	23
Figure 10. Heating rates for ten 5-km. layers computed from the temperature distributions in Figure 9.	24
Figure 11. Vertical speeds necessary to produce dynamic heating or cooling to compensate for heating rates shown in Figure 10.	26

List of Illustrations (cont'd)

	Page No.
Figure 12. Interpretation of location of thermal equator (doldrums) and subtropical high-pressure belts from planetary markings of Mars.	28

Background:

The material contained in this report has been presented before, in greater part, in a consultant report to McDonnell Aircraft Corporation in early 1966 (Bates, 1966), as well as in presentations to scientists at NASA-Langley Research Center and Jet Propulsion Laboratory in 1966. The soundings have been re-executed on an improved thermodynamic diagram which takes into account the variation of c_p and the adiabatic lapse rate with temperature. The results of the numerical radiation checks are of more recent origin, having been completed in late 1966.

Composition:

There is good observational evidence for two gases in the Martian atmosphere, viz: carbon dioxide and water vapor. The possibility exists for small amounts of other gases. It is evident, however, that two important and excellent observations have fixed carbon dioxide as the overwhelmingly predominant gas.

V. I. Moroz (Moroz, 1964) estimated that for the rotational fine lines of carbon dioxide in the 8700 Å region to be observed would require not less than 20 g cm^{-2} of carbon dioxide to be present in the Martian atmosphere. Since these were observed by Kaplan, Munch and Spinrad (1964) an amount of carbon dioxide of that magnitude or greater must have been present. If carbon dioxide were the only gas present the equivalent surface pressure -- in the martian gravitational field -- would be about 7.5 millibars.

The investigators of the Mariner IV occultation experiment (Kliore, Cain, Levy, Eshleman, Fjeldbo and Drake, 1965) computed a "surface" pressure of 5.7 millibars for a 100% carbon-dioxide atmosphere from data for the immersion portion of the experiment. This seemed at first glance to contradict the spectrometric observation. Assuming a "knife-edge" at about 3 km., however, for low-level cutoff of the microwave beam in the occultation experiment, the two experiments produce consistent results (See Fig. 1). This assumption provided the basis for an early involvement of a 100% carbon-dioxide atmospheric model in subsequent treatments and proved to be valid when computations of the emersion portion of the experiment became available.

The occultation point of Mariner IV was located, in immersion, at about 55°S and 177°W -- between Electris and Mare Chronium -- during late winter in the southern hemisphere of Mars. It is therefore likely that the surface pressure was somewhat above the equivalent-mean-sea-level pressure of the planet. A value of 7.0 millibars was therefore estimated for the latter. Since carbon-dioxide and argon are the heavier gases suggested for the Martian atmosphere; since a greater amount of carbon dioxide would require "knife-edge" heights beyond topographical variations otherwise deduced for the planet and lesser amounts would not permit the spectrometric observation obtained, it is estimated that the adoption of a 100% carbon-dioxide atmosphere with an equivalent-mean-sea-level pressure of 7.0 millibars is realistic within about $\pm 10\%$ for either value.

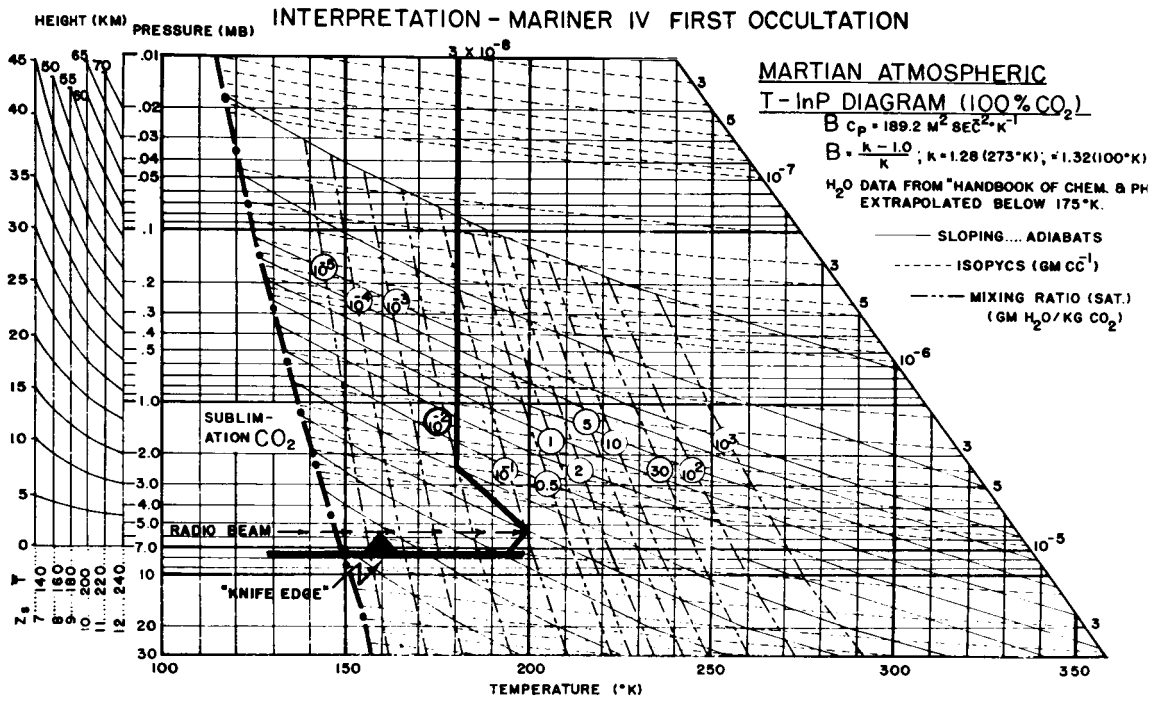


FIG. 1

The foregoing conclusions are consistent with the outgassing theory for the origin of planetary atmospheres if an accounting can be made for the low abundance of water vapor. The latter will be shown to be consistent with both the spectrometric estimate of about 14 ± 7 microns of precipitable water found by Spinrad and associates (Kaplan, Munch and Spinrad, 1964) and the thermodynamic structure estimated in this study -- viz: the Martian atmosphere contains an amount of water vapor consistent with its ability to hold water vapor and consistent with the absence of large water bodies or extensive ice fields on its surface. Thus, as a gaseous constituent of much significance in dynamic or radiation treatments in the homosphere -- as a gaseous constituent -- water vapor is eliminated. Since the outgassing theory notes an abundance of nitrogen that is about 3% that of carbon dioxide, that gas may also be neglected in further considerations.

Mean-Annual Subsolar-Meridian Surface-Temperature Distribution:

It will be useful to determine first some mean-annual distribution of temperature and pressure in sufficient depth in the Martian atmosphere based upon those observations and applicable deductions now available. From such a distribution one may then deduce seasonal and other deviations upon further observations and evidence.

The first distribution, logically, is that of surface temperature. Noting that radiometric observations have generally involved the central regions of the planetary disc under conditions of illumination, it is reasonable to identify these as subsolar-meridian values. Pettit (Pettit, 1961) has presented mean-annual values of surface temperature computed from such observations of 286°K at the equator and 211°K at the poles. Assuming a circulation regime similar to that of Earth (and this must be subsequently justified) the distribution of surface temperature between equator and pole may be approximated by:

$$1) \quad T_{\phi} = T_{\text{pole}} + (T_{\text{eq}} - T_{\text{pole}}) \cos \phi - a(T_{\text{eq}} - T_{\text{pole}}) \sin^2 \phi$$

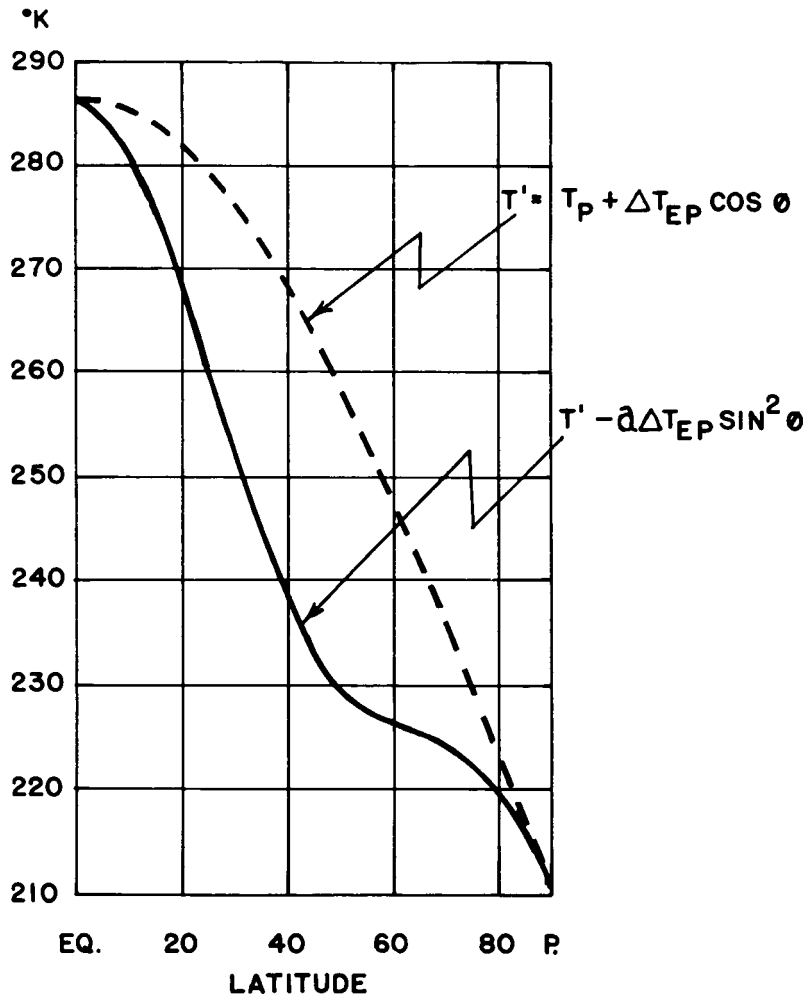
where: T_{eq} = observed equatorial temp.

T_{pole} = observed polar temp.

ϕ = latitude

a = an appropriate constant.

Utilizing continental-interior values of 305°K at the equator, 273°K at the pole and 284°K at 45° latitude for Earth yields a value of "a" of 0.41. Applying this value to 1) yields the estimated distribution shown in Fig. 2. The corresponding value at 45° latitude for Mars is 233°K -- close to the surface value used by Prabhakara and Hogan (Prabhakara & Hogan, 1965) in their radiation studies of the Martian atmosphere.



MEAN-ANNUAL SUBSOLAR-MERIDIAN
TEMPERATURE DISTRIBUTION - SURFACE.

FIG. 2

Depth of Troposphere:

The existence of an atmosphere which takes an effective part in maintaining the heat balance of a planet argues in itself some lower layer within which temperature, in the mean, decreases upward. Again, although the precise form and mechanics of the circulation may vary, the circulation contained in the lower layer will have some upper boundary, in the mean. It is necessary to estimate the depth of that layer before proceeding to an estimate of thermal structure in depth.

Limb observations of dust plumes rising from the surface in low latitudes indicate a height of about 30 km. for the troposphere in those regions if a convective (yellow-dust-devil) origin of such plumes is accepted (deVaucouleurs, 1954). Depths of cloud in the polar cloud caps, although more difficult to estimate from planet photographs (see, for example, Dollfuss, 1961 -- plates 22 November 1943, 0110 UT and 22 December 1943, 2142 UT), indicate a polar depth of troposphere of about 10 km. A mid-latitude depth of 20 km. seems realistic from the foregoing -- and it is also a value estimated as a mean value by many other investigators.

For the purpose of construction of a mean-annual subsolar-meridian cross-section, therefore, the depths of troposphere (ergo, heights of tropopause) estimated are: equatorial -- 30 km.; midlatitude -- 20 km.; and polar -- 10 km.

Lapse-rates of Temperature:

If convection is to exist in great depths in the equatorial regions, the lapse-rate of temperature on the subsolar meridian must be close to the dry-adiabatic lapse rate. An estimate of lapse rate in the polar region is more difficult. Noting, however, that this estimate in polar regions -- within reasonable limits -- has little effect on computations of mode of general circulation, and that the moist-adiabatic (pseudoadiabatic) lapse rate differs little from the dry-adiabatic lapse rate and, furthermore, that cloud exists over the poles for a long period of time, the dry-adiabatic rate is also selected for the polar troposphere. For midlatitude, a mean temperature of about 194°K is estimated from the range of mean tropospheric temperatures resulting from the lapse-rates argued at the equator and poles, viz: about 208°K at the equator and about 185°K at the pole, as follows:

$$2) \quad \bar{T}_{45} = \bar{T}_{eq} - (\bar{T}_{eq} - \bar{T}_{pole}) \sin 45^{\circ}$$

A surface temperature of 233°K and a mean-tropospheric temperature of 194°K yields a tropopause temperature of 155°K at midlatitudes and a lapse rate of 3.9°K km⁻¹ -- about 75% of the dry-adiabatic lapse rate used in these early computations, viz: 5.2°K km⁻¹. In view of the Earth-analogy used, the latter rate might be expected since it differs little from the standard-atmosphere-rate of-Earth equivalent.

Mode of the General Circulation:

Since an analogy to Earth has been argued in the foregoing it has been implied that the general circulation of Mars will be in the same mode, in the mean, as that of Earth. With an estimate of the mean-annual subsolar meridian mean-tropospheric-temperature difference, it is possible to test the validity of this assumption on two bases.

The first test bases upon the Hide-annulus experiment (Fultz, 1960) which has been previously presented by Tang (Tang, 1965). In this test the rotating-fluid system of the planetary atmosphere is scaled to laboratory results from a rotating-fluid experiment by means of Froude and Rossby (thermal Rossby) numbers. Since the results of the experiment are presented in terms of the inverse Froude number, this is first computed and found to be 4.5×10^{-3} . At that Froude number the planet will be in the wave regime (i. e. the regime similar to Earth with jet stream, typical circulation regimes or zones, migratory pressure systems, etc.), according to the laboratory experiment, if the Rossby number lies between about 0.04 and 0.12.

The Rossby number (thermal Rossby number) is computed from:

$$3) R_{ot} = \frac{g(\Delta T)H}{f^2 \bar{T} r \Delta r}$$

$$\text{where: } g = 3.8 \text{ m. sec}^{-2}$$

$$\bar{T} = 197^\circ\text{K (from values deduced above)}$$

$$H = 20 \text{ km. (mean of 30 km. and 10 km.)}$$

$$f = 7.1 \times 10^{-5} \text{ sec}^{-1} \text{ (Coriolis parameter at } 30^\circ \text{ lat.)}$$

$$r = 3.4 \times 10^6 \text{ m. (radius of Mars)}$$

$$\Delta r = 5.1 \times 10^6 \text{ m. (equator-pole distance)}$$

$$\Delta T = 23^\circ\text{K (from values deduced above)}$$

This yields a value of 0.10 for the Rossby number. Since this is within the range for the wave regime, the postulation of that mode of the general circulation is justified for the estimates of thermodynamic structure of the troposphere that have been made. In general, this may be interpreted as a mean-annual condition, since the nocturnal difference should be less than the subsolar-meridian, or noon, difference. This does not exclude the possibility of transitions to symmetric regimes during the year, but only that the mean mode for the planet during the year will be the wave regime.

Another check may be made through comparison with a critical value of total poleward heat flux computed by Mintz (Mintz, 1961), viz: 1.2×10^{11}

kilojoules sec^{-1} . If the value computed is less than this value, the mode of the general circulation should be the wave regime. Mintz suggests the following form for computation of a value for comparison:

$$4) \quad Q = \frac{\pi \, g k R \bar{T} \mu S^2}{1.414 \, \Omega^2}$$

where $g = 3.8 \, \text{m. sec}^{-2}$ (accel. of grav.)

$k = 1.3$ for CO_2 (ratio of sp. heats)

$R = 189.2 \, \text{m}^2 \, \text{sec}^{-2} \, \text{°K}^{-1}$ for CO_2 (sp. gas const.)

$\bar{T} = 197^\circ\text{K}$ (from values deduced) (mean temp. (troposphere))

$\mu = 10^{-2} \, \text{g m}^{-1} \, \text{sec}^{-1}$ (for CO_2) (coeff. of viscosity)

$S = 1 - \Gamma^{-1}$ (for midlatitudes, 0.23);

$\Omega = 1.4 \times 10^{-4} \, \text{sec}^{-1}$ (angular speed of planet).

The foregoing yields a value of 1.07×10^6 kj/sec. Since this is much less than 1.2×10^{11} a wave regime is again indicated. Even if eddy viscosity were substituted for the molecular viscosity in this expression -- increasing the result by a factor of from 10^3 to 10^5 -- a wave regime would continue to be indicated.

Note that the foregoing discounts the possibility of significant sinks or sources of gaseous mass in the Mars atmosphere due to sublimation or evaporation of carbon dioxide. Although it will be found that this process may proceed at various levels and times, evidence will be presented that the associated rates and total amounts are such as not to disturb the validity of the conclusions just reached.

Surface Pressure Distribution:

With increased confidence in a mean wave regime the analogy to Earth may be extended to a gross estimate of the latitudinal distribution of surface pressure. Typical circulation zones may be expected, viz: (1) a belt of light winds near the equator, or doldrums, extending about 5° latitude to the north and south; (2) trade-wind belts extending from about 5° to 20° latitude in each hemisphere; (3) subtropical high-pressure belts extending from about 20° to 35° latitude; (4) a westerlies belt extending from about 35° latitude to a polar-front zone centered around 60° latitude, the latter extending to about 75° latitude in longitudinal deviations; and (5) a polar high with associated easterlies.

The surface pressure variation between these zones of Earth, in the annual mean, is approximately from 1030 millibars to 996 millibars, or a variation of

about $\pm 1.7\%$ about the mean of 1013 millibars. Other estimates, which will be presented, indicate a circulation for the planet, Mars, about two and a half times as intense as that of Earth. This may be accounted for in various ways -- a smoother, homogeneous surface, larger mean thermal contrasts, etc. A variation of surface pressure between zones in the annual mean of about $\pm 4.3\%$ is therefore estimated. With an equivalent-mean-sea-level pressure of 7.0 millibars, this is equivalent to a range of ± 0.3 millibars. It is also roughly equivalent to a zonal mean speed in the range 20 to 25 m sec⁻¹ for surface wind.

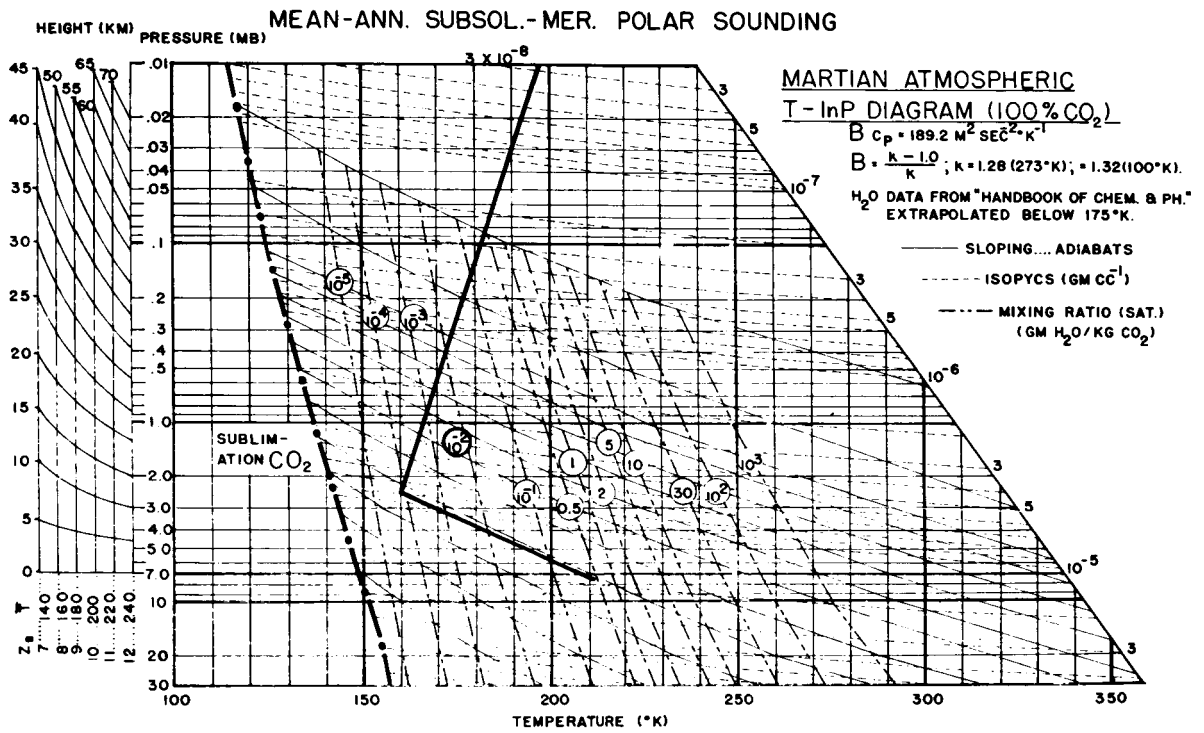
A scale height value of about 8.8 km. (mean temperature of about 175°K) was used to extend the midlatitude sounding to about 49 km. at 0.03 millibars. This is consistent with the Mariner IV occultation experiment. It should be noted that great deviations, either temporal or spatial, should not be expected from the values observed, viz: 9 ± 1 km., in a deep column in the Martian atmosphere. With slight correction to hold the pressure surface of 0.03 millibars at 49 km., the equatorial and polar soundings were similarly extended. The surface of 0.03 millibars was chosen as the threshold of non-significant pressure-magnitude variation at the surface. The assumption of a pressure surface coincident with an areopotential surface at 0.03 mb. (i. e., level) is not too bad, especially for the foregoing purpose. Only slight deviations from this condition leads quickly to extreme wind conditions either at the surface or aloft -- and, conversely, extreme wind conditions at either level do not disturb the soundings so fitted in the deep column by large magnitudes. The assumption of hydrostatic balance in these vertical temperature distribution estimates is rather well justified by the deduced wave regime, Earth similarity and various direct observations of the mean condition of the Martian atmosphere.

The resultant mean-annual subsolar-meridian soundings are shown, respectively, in Figures 3, 4 and 5.

Aspects of the Equatorial Sounding:

It is interesting to note that the tropopause temperature is close to the sublimation curve of carbon dioxide. In excursions of surface temperature above the mean-annual subsolar-value of 286°K adopted in its construction, carbon-dioxide sublimation could be definitely expected. Although this sounding was based upon an assumed constant dry-adiabatic lapse rate of 5.2°K⁻¹ -- and the correct rate is shown by the dry-adiabats (solid lines sloping downward to right) on the improved thermodynamic diagram -- so that the tropopause temperature should actually be near 147°K, occasional excursions to carbon-dioxide sublimation conditions should be expected at the equatorial tropopause. These excursions would not be expected to produce deep clouds of carbon-dioxide crystals which would be opaque at all visible-light wavelengths -- as might be expected in some extremely-cold columns suggested for the Martian atmosphere -- but could account, at least in part, for the tenuous, small-particulate cloud which may be responsible, at least in part, for the observed "blue haze".

One might also note that if only 1°K temperature differential of the initial low-level 8°K temperature differential between light and dark areas



is effective through a depth of 20 km., an updraft speed of about 25 m/sec could be attained in a yellow-dust devil at that altitude with an overshoot to 30 km. not at all unlikely.

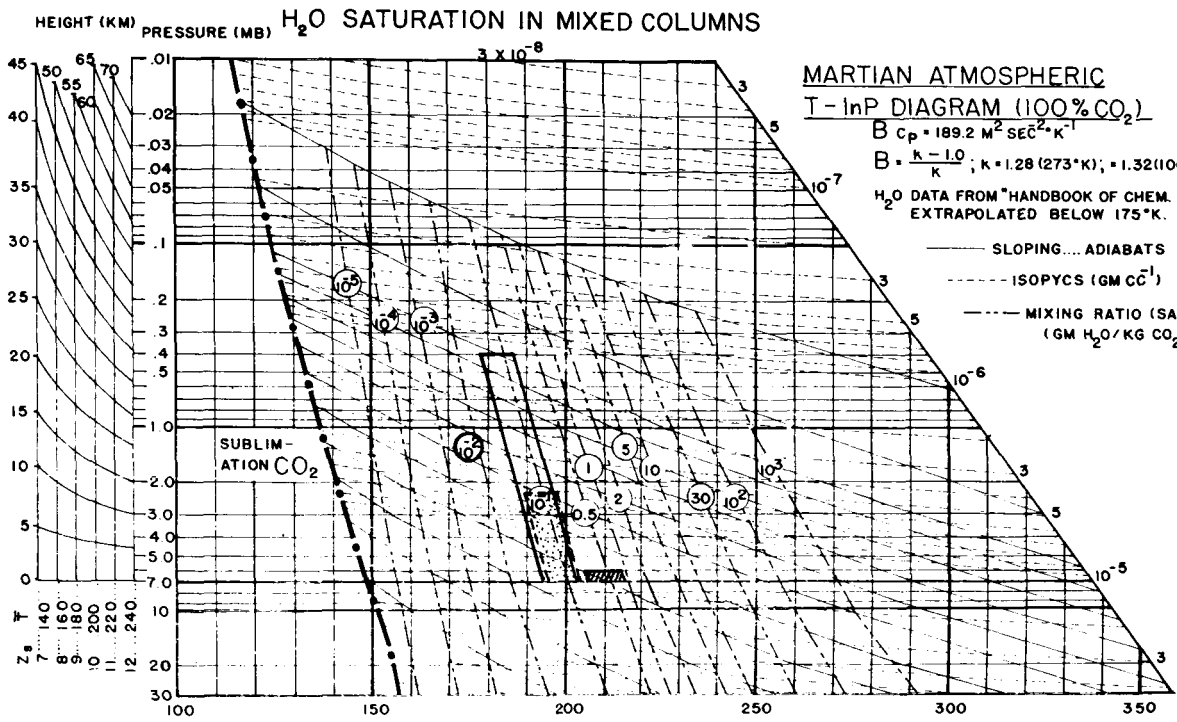
Water Vapor in Mixed Columns:

It will be noted that mixing-ratio isopleths have been constructed on the thermodynamic diagram used as a base for several of the figures. These isopleths are based upon vapor pressures at saturation from a standard reference down to 175°K and are estimated from a second-order extrapolation of those values down to 139°K. The bold label on the 10^{-2}g kg^{-1} isopleth marks the temperature of 175°K below which the data is less reliable.

If the equatorial or the midlatitude tropospheric columns are mixed in depth in the troposphere and the water vapor is assumed to be contained in the troposphere, the range of mixing ratios (ergo, dew point temperatures) shown by the tall column (Fig. 6) will result. Due to the small mass above 20 km. there is little difference in mixing through a greater depth. These ranges correspond to the range 14 ± 7 microns of liquid water found by spectrometric observation. Mixing in the smaller depth of the polar column results in the column identified by stippling, and mixing in a column of one kilometer results in the black column. It is interesting to note that this range of water contained in the column over the great range of mixing depth results in a dew-point-temperature range of only 192°K to about 213°K. Other vertical distributions -- other than a shallow surface layer in active condensation and deposition -- will result in higher dew point temperatures at low levels. Since these dew point temperatures are warmer than minimum temperatures deduced at any latitude, the fate of the water vapor which might be expected to be present in the Martian atmosphere is apparent, if the outgassing origin of the atmosphere is valid. It has gone hence, because it could not be contained in the temperature range deduced. The absence of large liquid or water surfaces -- both from direct observation and the great dryness of air columns which could contain a great deal more water if exposed to such interfaces -- seems to argue the retreat of the huge amount of water that may be estimated from the outgassing theory to subaresian deposits locked away from atmospheric contact or its escape (possibly, decomposition and escape) in the early evolution of the atmosphere.

In any case, the extreme aridity of the equatorial and subtropical atmosphere should be borne in mind in studies of dust and surface materials, as well as in engineering of the vehicles and devices planned for exploration of Mars. Relative humidities in the range of hundredths of one percent will be typical. In the absence of water compaction, dust particles of one micron or less in size are not unlikely on the Martian surface and in suspension in the Martian atmosphere.

It should also be noted that, at any level, before sublimation of carbon dioxide will proceed condensation or sublimation of water vapor must take place. It is unlikely that clouds of pure carbon dioxide, or depositions of pure carbon dioxide, exist on Mars. Attention should therefore be directed toward mixtures and mixed deposits of carbon dioxide and water.



Aspects of the Mid-Latitude Sounding:

The 45°-latitude sounding shown in Figure 4 might be thought of as similar to the "standard atmosphere" of Earth. Thus, equivalent STP would be 233°K and 7.0 millibars with "standard" density of $1.6 \times 10^{-5} \text{ g cm}^{-3}$. With respect to the mean water-vapor conditions previously deduced and shown in Figure 6, it should be noted that this column is also extremely dry at low levels at subsolar-meridian time -- even when the upper bound of the indicated range is determined by mixing through one kilometer (dew point temperature of about 213°K). The indicated relative humidity for that condition is about 1%. Note, however, that saturation is indicated in the diurnal range at low levels, and that mixing in depth -- for cases of deviation to dry-adiabatic lapse rate of temperature -- should produce clouds. The foregoing seems to realistically fit observations in these latitudes -- i. e. occasional white clouds in the warm season, low-latitude boundary of polar cloud cap in winter, evidence of low-level cloud on the morning limb with additional evidence of precipitation or direct condensation in observations of transient patches of "frost" on the surface.

Aspects of the Polar Sounding:

It should be noted that this sounding shown in Figure 5 saturates in the mixing-ratio range of the accepted mean range of water vapor in the Martian atmospheric column. It should therefore be expected that clouds will be frequent over the polar regions, with essentially a continuous cloud cover in winter. Note that a mean-annual subsolar-meridian sounding for the pole is actually merely a mean-annual sounding. Deviations of a seasonal nature must be determined before a useful study of the mechanics of these clouds and the associated precipitation or surface deposition of water and, possibly, carbon dioxide can be conducted. The possibility of temperatures sufficiently cold as to permit sublimation of carbon dioxide in winter is not excluded by a mean surface temperature of 211°K. It is rather certain, however, that condensation and depositon of water hydrometeors must precede sublimation and deposition of carbon-dioxide -- and if the latter occurs there will be a mixture of water and carbon dioxide precipitates in the deposit. Theoretical and experimental studies of the Martian polar "ice" caps should involve the foregoing.

Some Circulation Estimates:

The value of 0.10 for Rossby thermal number computed in a previous section not only yields the result of the mean wave-regime circulation for Mars from analogy to the Hide-annulus experiment, but also indicates a wave-number of 3 as a mean condition for Mars. This is a "high-index" condition, i. e. one typified by rapidly-moving, open-wave cyclones and generally fair weather on Earth.

It is possible to translate this into an estimate of the speed of the zonal westerlies aloft from the Rossby long-wave equation, assuming a stationary long-wave pattern, viz:

$$5) \quad U_{m \text{ stat}} = \frac{2\Omega r \cos^3 \phi}{N^2}$$

where r = Mars radius

N = wave number (number in hemisphere)

ϕ = latitude (here, 45°).

This yields a value of 19.0 m sec^{-1} at a level of non-divergence which is approximately at one-third the depth of the troposphere. Assuming linear variation of speed with height this would yield a jet-stream speed of about 57 m/sec. , and a mean tropospheric speed of about 28 m sec^{-1} .

Since the typical long-wave number of Earth is 4, we may also check the foregoing in a comparison of the mean jet-stream speeds. An estimate of Earth's mean jet-stream is obtained from the cross-sections of Hess (e. g. Hess, 1950), viz: core speed of about 38 m sec^{-1} . The interrelationship from the Rossby long-wave equation should be:

$$6) \frac{V_{j \text{ mars}}}{V_{j \text{ earth}}} = \frac{(N_{\text{earth}})^2}{(N_{\text{mars}})^2} = 1.78$$

Which yields a value of about 67 m sec^{-1} , slightly greater but consistent with the foregoing value.

Mean-Annual Subsolar-Meridian Cross-Section:

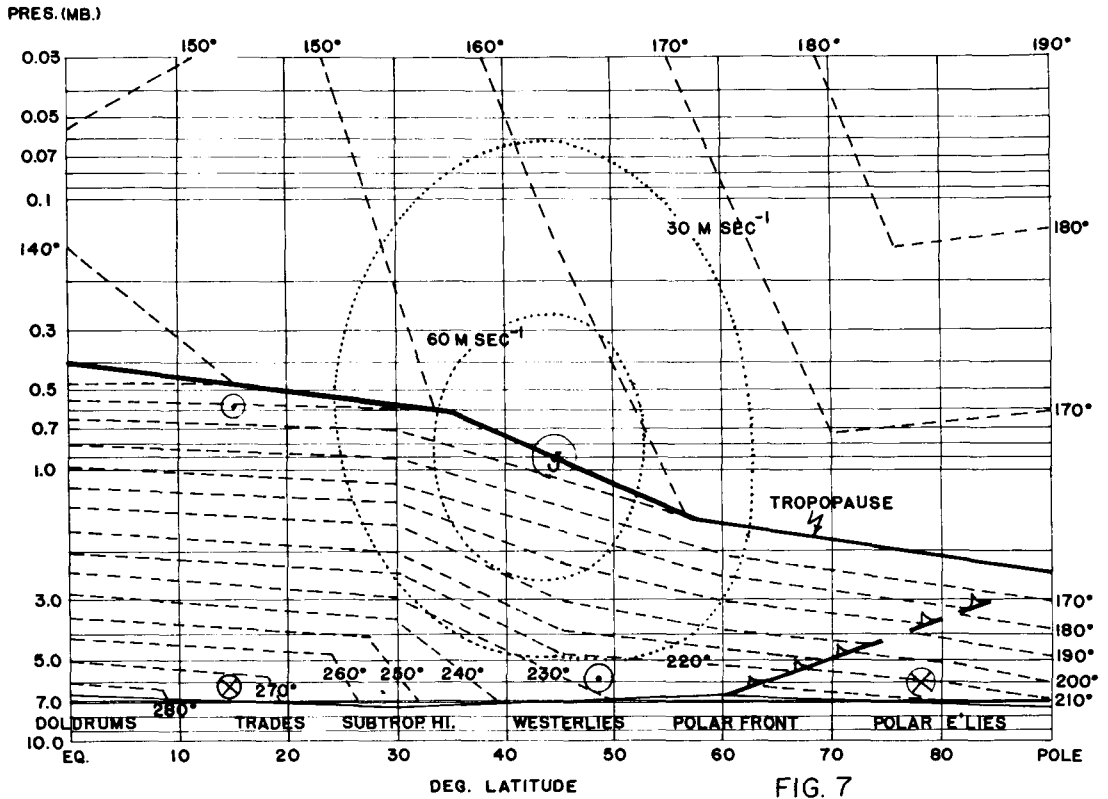
Assuming a jet-stream at 20 km. (midlatitude tropopause height) and 45° latitude, the soundings derived for the three latitudinal positions are utilized to construct a first approximation to a mean-annual subsolar-meridian cross-section. The isotherms are adjusted to an approximate thermal-wind fit to the isotachs of zonal speed shown. The surface points are adjusted to the surface pressures deduced for the several zones noted before. The cross-section is shown in Figure 7.

This cross-section assumes hemispheric symmetry in seasonal effects, e. g. insolation. Since the Southern Hemisphere is much warmer than the Northern Hemisphere in its summer (closer to sun), it can be expected that there will be a southward shift in the mean position of the heat equator and, therefore, the doldrums. A similar sense of shifting can be expected for other features, e. g. the subtropical highs. A tentative basis for estimating the magnitude of this asymmetry will be suggested in a later section.

Storm and Local Circulations:

Two principal storm types may be anticipated for Mars, viz: extratropical cyclones and yellow-dust devils. A third event, which might be thought of as a storm event, may occur in the major yellow-dust lifting in the Southern Hemisphere in summer, especially during years of sunspot activity. The latter may be related to a transition in the general circulation mode itself.

MEAN-ANNUAL SUBSOLAR-MERIDIAN CROSS-SECTION: MARS



From the wave number of three deduced as a mean condition for the wave regime, the extratropical cyclones may be expected to be similar to those of Earth during high-index conditions, viz: rapidly-moving, open-wave cyclones. A central pressure of about 1004 millibars in a storm of about 300-km. diameter would be typical of Earth. A central pressure of 986 millibars in a storm of similar size would be an extreme limiting case. Scaling these to Mars yields an estimate of pressure gradients ranging from about 5×10^{-4} mb km⁻¹ to 1.5×10^{-3} mb km⁻¹, which corresponds to a range of speeds from 30 m sec⁻¹ to 90 m sec⁻¹. Since the analogue magnitudes from Earth are conservative and these wind speeds are geostrophically estimated, these estimates are quite generous.

The terrestrial dust devil is probably the most likely analogue to the yellow-dust devil of Mars. Conservatively, an analogy may be made to the tornado of Earth. Accepting the extreme estimate of about 450 knots as a maximum speed in the tornado, a pressure differential of approximately 300 millibars in a no-loss conservation-of-moment-of-momentum process to attain that speed (environment-funnel pressure differential) and scaling this to Mars, yields a pressure differential of about two millibars and a related speed of about 155 m sec⁻¹.

The organization of the circulation leading to the more general yellow-dust events, such as occurred in the Southern Hemisphere summer of 1956, is uncertain. A current estimate of the threshold of yellow-dust lifting -- and a great deal of further research is required for confidence in any estimate of this magnitude -- is about 100 ft sec⁻¹ or, for practical purposes, 30 m sec⁻¹. The possibilities seem, therefore, to be extratropical cyclones, yellow-dust devils or equivalent "gradient" winds in an intense symmetrical regime.

The lack of marked topographical relief on Mars probably excludes intense fall-winds. The possibility of circulations of different or more-intense nature than on Earth at the polar-cap boundaries and in the process of sublimation and evaporation of carbon-dioxide in the polar-caps cannot be excluded. It is also possible that vigorous limb circulations (morning and evening freshening of wind) may exist in association with a diurnal wave. The latter, however, from astronomical evidence does not appear to lead to a general yellow-dust lifting.

The infrequency of yellow-dust clouds in astronomical observations permits the possibility of exclusion of the related extreme surface wind speeds from involvement in design of exploratory entry vehicles. For example, choosing the yellow-dust devil as the agent for all significant and perceptible lifting of yellow-dust, estimating a related area of the vortex of about 64×10^6 m² (8 to 10 km. in diameter) and a mean duration of 4 hours and further generously estimating the occurrence of 1200 of these vortices annually, a time-area product of about 3.1×10^{11} m² hr. is indicated. Relating this to a planetary area-time of about 2×10^{17} m² hr. yields a probability of about 1.5×10^{-6} of intercepting a vortex in random entry -- i. e. a risk in the range of chances in a million. The foregoing is a conservative estimate. Further careful studies of astronomical observations of the yellow-cloud events, the mechanics of yellow-dust lifting and wind speeds associated with yellow-dust lifting should permit more confident estimates of this type.

The mechanics of yellow-dust lifting have been most confidently observed in limb observations. A mode of lifting that has been observed reveals a column (interpreted as a yellow-dust devil) in the winter hemisphere (about 10° to 15° from the equator) extending upward through the tropical troposphere. The dust cloud appears and spreads from this source, being carried in inertial flow into the summer hemisphere and entering into the westerlies of that hemisphere. Tang (Tang, 1965) has suggested this lifting as occurring along a cold front, but the source in the winter hemisphere and the mechanics of frontal surfaces in equatorial regions would seem to exclude that mechanism.

In the spectacular yellow-dust-cloud event of 1956 the desert, Hellas, was observed to disappear (darken), subsequently reappearing. In that event alone there is good evidence for the source of yellow clouds in wind-lifted dust. There is also a good basis for the interpretation of mean surface-wind regimes from planetary markings.

Surface-Wind-Speed Probabilities in Random Entries:

From the estimate of mean wind speeds of 20 to 25 m sec⁻¹ in the trades and in the westerlies-polar-front zone and lighter mean wind speeds in the doldrums, subtropical high-pressure belts and polar highs, it is possible -- utilizing Earth analogy and the storm and local speed estimates in the foregoing -- to make a first crude estimate of the probability of sampling a given surface wind speed in a random entry into the Martian atmosphere. See Figure 8.

Estimates were first made for probability distributions within each of the zones indicated. These were then weighted for the relative planetary area occupied by each zone and summed in the class intervals. The bases for estimates in each zone are conservative, e. g. the frequency and area of extratropical cyclones in the westerlies and polar-front zone.

Estimates of Lateral (Meridional) and Vertical Speeds:

An estimate of mean lateral (meridional) speed may be obtained through an adaptation of methods evolved by Haurwitz in his basic text (Haurwitz, 1941). Note that the method used here, though similar to that involving equatorial-polar heating-rate difference (e. g. Tang, 1965), is not identical to that method. In the determination of V, the meridional speed, the equatorial-polar-temperature difference will be utilized. In addition, in determining the "braking action" on the circulation of the Coriolis force of the westerlies and the viscous force on the meridional speed, appropriate lengths (and not total lengths) of the line of integration will be used.

The acceleration of circulation along a closed line of height equal to the tropopause height and length equal to the equatorial-polar distance may be expressed for a non-viscous fluid in a non-rotating system as:

$$7) \quad \dot{C} = R(\bar{T}_{eq} - \bar{T}_{pole}) \ln\left(\frac{P}{P_T}\right)$$

PLANETARY SURFACE-WIND-SPEED PROBABILITY ESTIMATES: MARS

BY ZONES AND FOR PLANET, BASED ON ZONE AREA (% OF PLANET AREA),
ESTIMATED PROBABILITY DISTRIBUTIONS WITHIN ZONES.

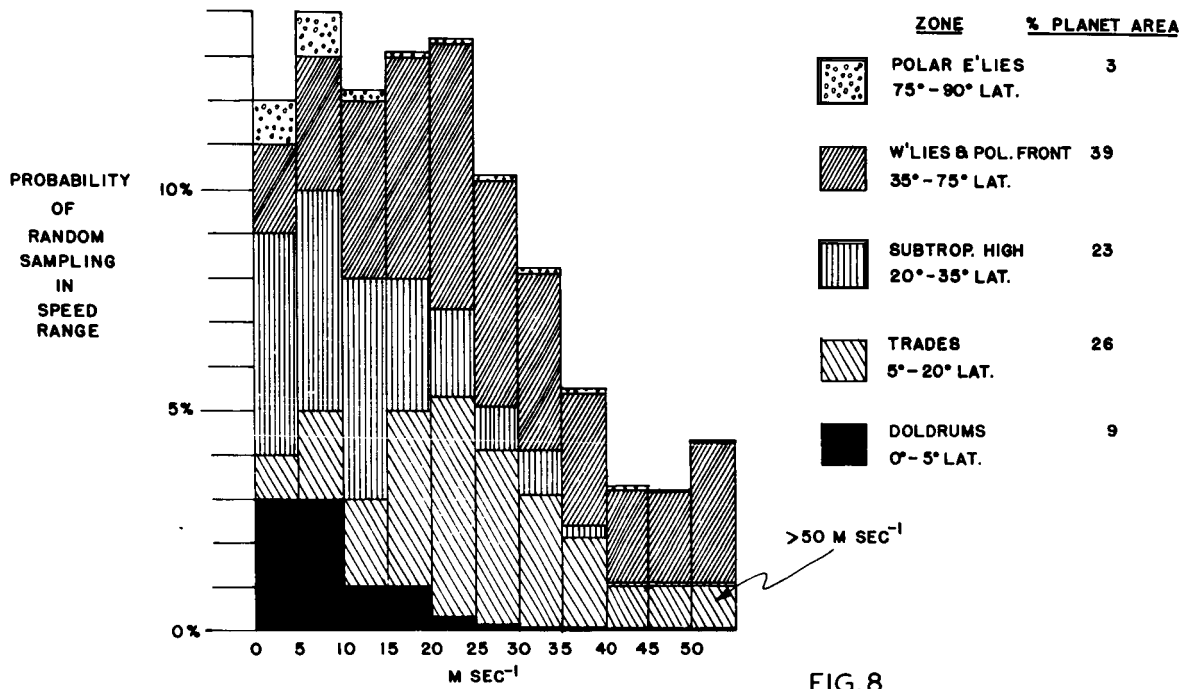


FIG. 8

where: \dot{C} = acceleration of circulation;

P_0 = surface pressure (here, 7.0 mb);

P_T = tropopause pressure (here, 0.9 mb);

$\bar{T}_{eq} - \bar{T}_{pole}$ = equator-pole mean-tropospheric temperature difference.

Since, over the long-time mean the acceleration of circulation must be zero, this acceleration is countered principally by the action of the Coriolis force of the westerlies and the viscous force due to the meridional speed -- each acting on an appropriate portion of the closed line.

The foregoing may be expressed:

$$8) \quad \dot{C}_{decel} = kV(\Delta S)_U + fU(\Delta S)_V$$

where: k = an appropriate drag coefficient
(here, taken as 10^{-5} sec^{-1});

f = Coriolis parameter (here taken at 45° lat.);

U = mean speed of westerlies;

V = mean meridional speed;

$(\Delta S)_U$ & $(\Delta S)_V$ = appropriate portions of the closed curve of integration with appropriate senses.

In determining the latter, it must be borne in mind that the westerlies will contribute aloft along the equator to pole segment and over the meridional extent of the westerlies (about 55° lat.). Similarly, the viscous force of the meridional flow will contribute at low levels along the pole to equator segment and in the regions outside the light, variable winds of the doldrums, subtropical highs and polar highs (or, again, over about 55° of latitude).

Haurwitz has also suggested (Haurwitz, 1962) that the viscous force of the westerlies is approximately balanced by the Coriolis force of the meridional flow, or:

$$9) \quad U = \frac{fV}{k}$$

Combining 7), 8) and 9), taking $(\Delta S)_U = (\Delta S)_V = 3.2 \times 10^6 \text{ m.}$:

$$10) \quad V = \frac{R(\bar{T}_{eq} - \bar{T}_{pole}) \ln\left(\frac{P_0}{P_T}\right)}{k\left(1 + \frac{f^2}{k^2}\right) \Delta S}$$

Introducing the equator-pole mean-tropospheric temperature difference of 23°K previously estimated and other variables as before or as noted yields:

$$V = 2.8 \text{ m sec}^{-1}$$

and, from 9):

$$U = 28 \text{ m sec}^{-1}$$

which agrees with the mean-tropospheric-westerly speed previously deduced.

The foregoing method eliminates the necessity of a further estimate of heating-rate differential -- a difficult estimate a priori -- as in the method applied by Tang (Tang, 1965).

Estimate of the mean-tropospheric vertical-speed magnitude may be obtained from the continuity equation in the form:

$$11) \quad \rho_{LT} V A_V = \rho_T \bar{w}_u A_u = \rho_T \bar{w}_d A_d$$

where: ρ_{LT} is mean density for the lower troposphere (about $1.0 \times 10^{-5} \text{ g cm}^{-3}$);

A_V is cross-sectional area along a parallel and for half the depth of troposphere at 45° lat. ($1.55 \times 10^{11} \text{ m}^2$);

\bar{w}_u is mean upward vertical speed;

ρ_T is mean tropospheric density (about $7 \times 10^{-6} \text{ g cm}^{-3}$);

A_u is approximate area with mean upward vertical motion (about $1.7 \times 10^{13} \text{ m}^2$);

\bar{w}_d is mean downward vertical motion;

A_d is approximate area with mean downward vertical motion (about $4.6 \times 10^{13} \text{ m}^2$).

The foregoing yields upward vertical speeds in the range 3 to 4 cm sec^{-1} , and downward vertical speeds in the range 1 to 2 cm sec^{-1} . These are gross space-time mean values.

Vertical motions in extratropical cyclones may be expected to exceed these by an order of magnitude, i. e. to be in the range 10 to 40 cm sec^{-1} . In the yellow-dust devil, upward speeds in the range 10 to 100 m sec^{-1} may be expected in the lower troposphere.

Radiation Checks on Estimated Soundings:

A numerical formulation of a basic technique developed by Pallmann (Pallmann, 1966) has been utilized to compute heating rates in ten 5-km. layers for any given fixed temperature distribution. This method takes into account effects of absorption by carbon dioxide in the near infra-red in incoming solar radiation, as well as the usual absorption in the far infra-red by carbon dioxide in outgoing and inter-layer radiation.

The net flux at eleven layers is computed as the difference between incoming (negative) and outgoing (positive) fluxes from:

$$12) F_-(x_o) = \pi \sum_{i=1}^N \Delta n_i \left[\sum_{m=1}^L B_{n_i}(x_m, n_i) \frac{\Delta J_F[(x_o - x_m), n_i]}{\Delta x_m} \Delta x_m \right] \\ + \frac{2}{\pi} \sum_{k=1}^M E_o^S(n_{ki}, 0^\circ \text{lat}) J[(x_o - 0), n_k] \Delta n_k$$

and:

$$13) F_+(x_o) = \pi \sum_{i=1}^N \Delta n_i \left[\sum_{m=1}^L B_{n_i}(x_m, n_i) \Delta J_F[(x_m - x_o), n_i] \right] \\ + \pi \sum_{i=1}^N \Delta n_i B_{n_i}(x_s, n_i) J_F[(x_s - x_o), n_i]$$

The above formulations and meanings of terms may be better seen in the numerical formulation and program given in the appendix. Note, however, that the contribution from direct solar radiation through the layers above, as well as contributions from the layers above, is taken into consideration in 12). Similarly, the contribution from the surface through the layers below, as well as the contributions from the layers below, is accounted for in 13). No attempt is made in this first approximation to account for scattering of or for cloud effects.

The net fluxes at the layer boundaries are then used to obtain flux divergence or convergence in each layer, and these are converted into heating rates for the carbon-dioxide atmosphere. In the long-term mean the resultant radiational heating rates must be compensated by dynamic (vertical-motion) heating or cooling or by advective heating or cooling. The test applied here is that of dynamic heating or cooling to determine if the resultant vertical speeds are of a reasonable order of magnitude.

The sounding tested is the 45^o-latitude mean-annual subsolar-meridian sounding described before (curve marked "Bates" in Figure 9). It is inter-compared with suggested temperature distributions with height by other investigators (note that this tests only the temperature distribution with

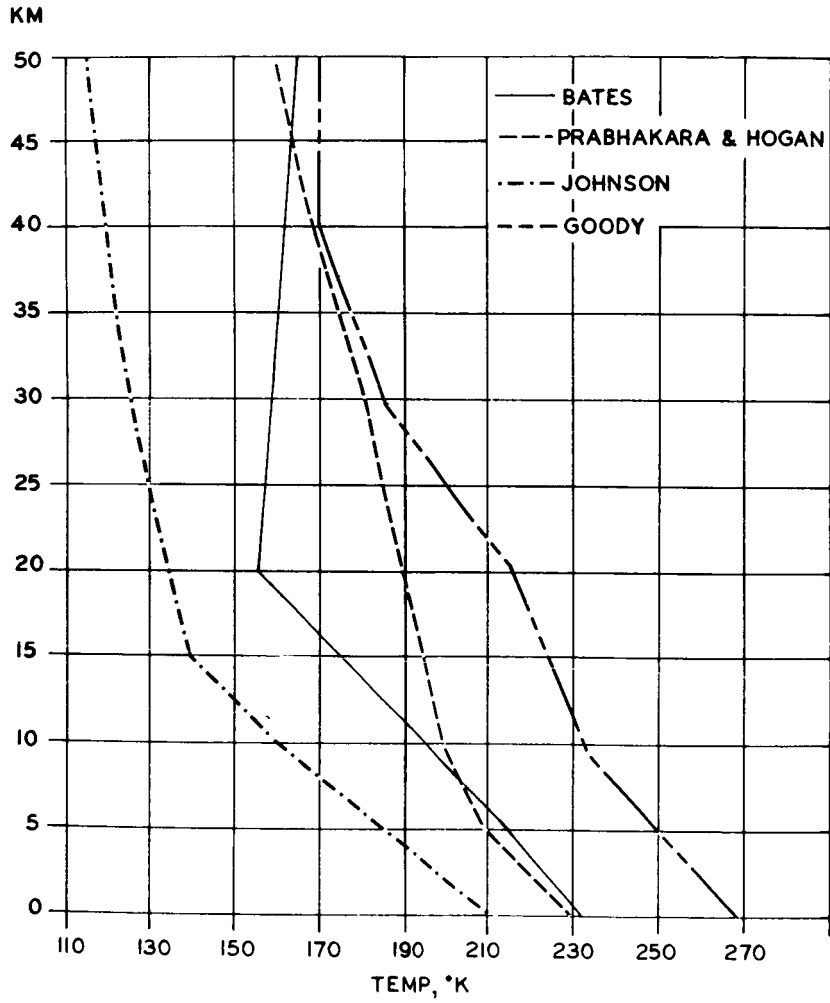


FIG 9
SEVERAL TEMPERATURE DISTRIBUTIONS IN DEPTH SUGGESTED
FOR MARTIAN ATMOSPHERE

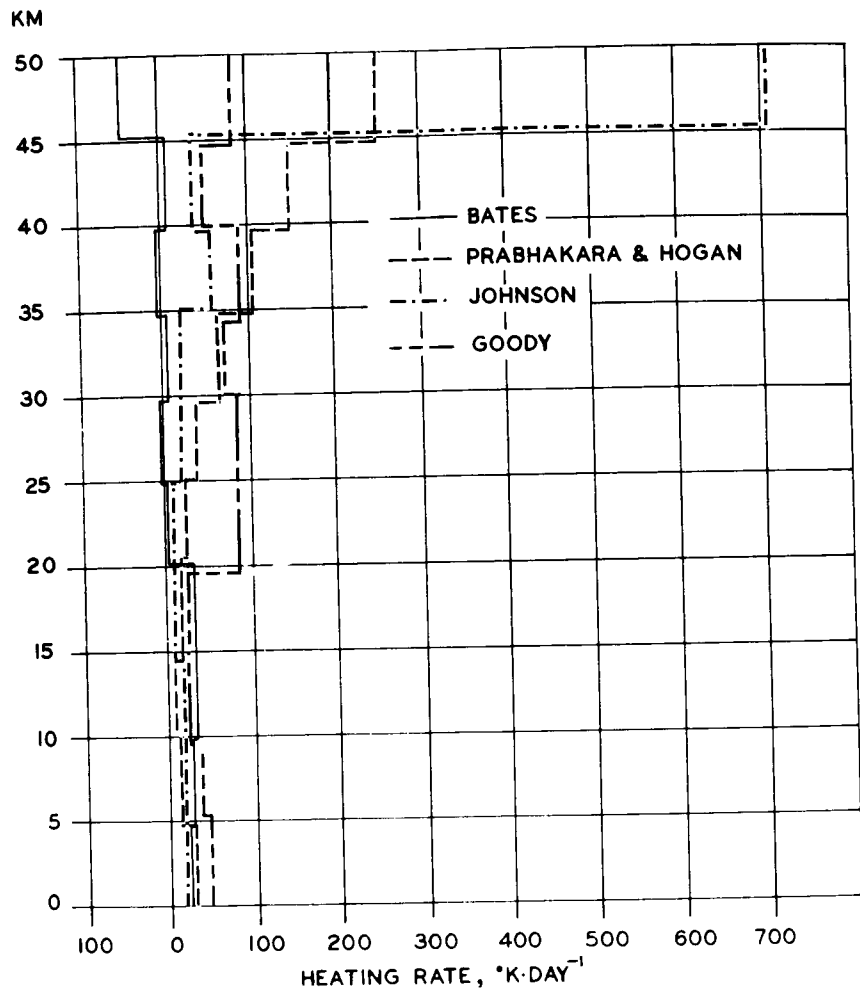


FIG 10
HEATING RATES RESULTING FROM RADIATION SOLUTIONS

height and not the total models suggested by those investigators). The distributions of Johnson (Johnson, 1965) and Goody (Goody, 1964) constitute "coldest" and "warmest" columns. The distribution of Prabhakara & Hogan (1965) is included as the closest similar computation with respect to constituents, surface pressure, etc. The foregoing are also shown in Figure 9.

The heating-rates solutions for each of these distributions (for 100% CO₂ atmosphere, 7.0 millibar surface pressure, etc.) are shown in Figure 10.

The magnitudes of vertical motion required for compensation in dynamic heating or cooling are shown in Figure 11. These are computed from:

$$14) \quad \bar{w} = \frac{\text{Heating rate of layer (}^{\circ}\text{K/sec)}}{\Gamma_d - \Gamma_{\text{layers}}}$$

In mean magnitudes of related vertical motions required for compensation all soundings fall within reasonable limits for a first approximation -- in spite of the extreme values obtained for the upper 10 kilometers (where other processes may be acting in compensation in the very tenuous atmosphere). It is encouraging to note, however, that the magnitude of 10 cm sec⁻¹ obtained for the 45°-latitude mean-annual subsolar-meridian sounding is closest to the ambient range of vertical motions previously deduced.

Deduction of Circulation from Planetary Markings:

It seems reasonable to relate differences in planetary markings on Mars to differences in lifting and in depositon of yellow-dust by the winds of the planet -- at least in part. The probable nature of the desert, Hellas, as a layer of dust deposited over underlying dark marking has been indicated in its disappearance and reappearance in the spectacular yellow-dust event of 1956.

If one would then assume an underlying dark marking for the entire planet -- whatever its physical or geological (better, areological) nature -- the bright areas, or deserts, should then be preferred regions for dust deposition. It follows, therefore, that these should be regions typified, in the mean, by lighter low-level winds and by subsidence (sinking motion) in the troposphere. A corollary to this -- admitting also the possibility of greater surface roughness as a factor in the lifting of dust -- is that dark area should be regions of stronger surface winds in the mean and upward vertical motions.

Using the MEC-1 prototype Mercator projection of Mars published by the U. S. A. F. Aeronautical Chart and Information Center, an approximate delineation of bright (dashed line) and dark areas (dotted line) of Mars

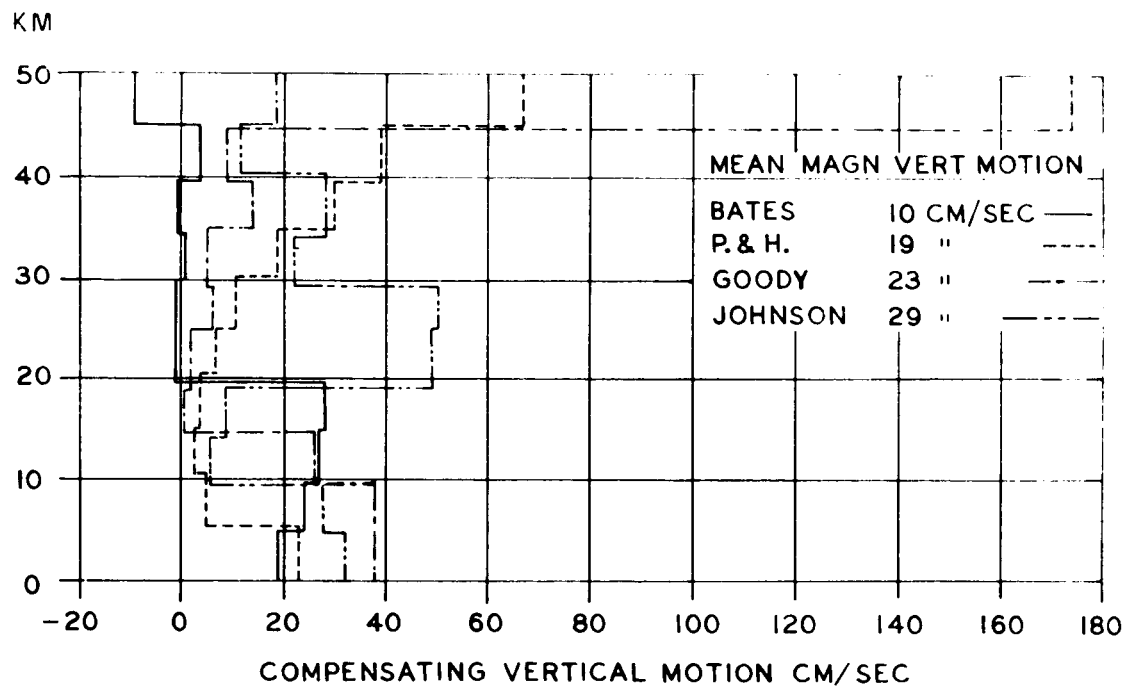


FIG. 11:
 VERTICAL MOTIONS REQUIRED TO
 COMPENSATE HEATING RATES SHOWN IN FIG. 10.

has been made in Figure 12. If the "heat equator" of the planet is shifted to 15°S, the Southern-Hemisphere subtropical high-pressure belt to 45°S and the Northern-Hemisphere subtropical high-pressure belt to 25°N, a surprising goodness of fit of the deduced circulation zones to dark and bright areas may be noted. The heat equator then centroids the belt of darkest markings on the planet, and the subtropical high-pressure belts coincide with the centerlines of the deserts in both hemispheres. Such a shift may be anticipated because of closer proximity to the Sun in Southern Hemisphere summer. Thus, a first basis for estimating interhemispheric asymmetry of the distribution shown in Figure 7 is deduced.

Another interesting aspect of this interpretation of planetary markings may be found in the relative positions of Mare Acidalium and the darker markings north of Isidis Regio (northward extension of Thoth-Nepenthes). The centroids of these darker areas in the vast bright areas of the Northern Hemisphere are located at about 30°W and 90°E, respectively -- or 120° longitude apart. This is the wave-length of a three-wave pattern of the long waves in the hemisphere. If the dark markings may be attributed to a greater relative frequency of extratropical cyclones (ambient condition of higher wind speeds and upward vertical motions) these dark areas may connote the presence of "action centers" similar to the Aleutian and Icelandic "lows" of Earth.

The southward shift of the subtropical high-pressure belt and trades of the Northern Hemisphere would also account for the observed interhemispheric inertial flow from the Northern to the Southern hemisphere at the altitudes of the yellow-dust events.

The implications of the foregoing in increasing knowledge of the structure and circulation of the Martian troposphere through further careful studies of astronomical observations and, possibly, in extending knowledge of the nature and materials of the Martian surface must be obvious.

Current Estimates of Atmospheric Magnitudes:

Accepting the occultation and spectrometric observations upon which the foregoing has been principally based at a high level of confidence, it is possible to estimate some useful magnitudes.

It is suggested that the surface conditions found for the midlatitude mean-annual subsolar-meridian sounding are similar in nature to "standard pressure and temperature" (STP) conditions for Earth. Assigning, conservatively, twice the zonal pressure variation deduced and the error intervals indicated for the occultation experiment in temperature and scale height, the suggested equivalent STP conditions for Mars are:

$$\text{Pressure} = 7.0 \pm 0.6 \text{ millibars}$$

$$\text{Temperature} = 233 \pm 20 \text{ }^\circ\text{K}$$

$$\text{Scale Height} = 9.8 \pm 1 \text{ km. (midlatitude troposphere).}$$

$$\text{Density} = (1.58 \pm 0.30) \times 10^{-5} \text{ g cm}^{-3}$$

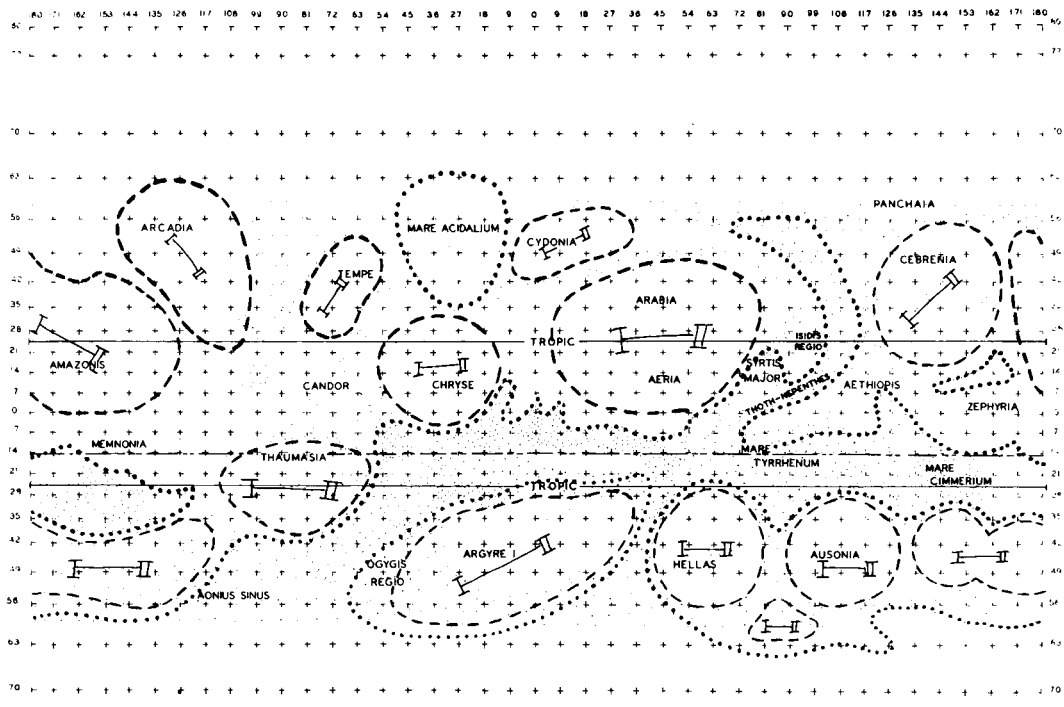
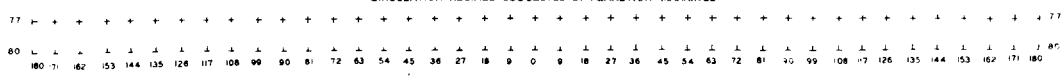


FIG. 12
CIRCULATION REGIMES SUGGESTED BY PLANETARY MARKINGS



From the distribution in Figure 8, mean surface (gradient level) wind speed for Mars is estimated as:

$$\bar{V} = 20 \pm 10 \text{ m sec}^{-1}$$

Reasonably excluding the yellow-dust devil circulation from consideration and noting the conservative nature of the distribution in Figure 8, it is suggested that a speed three standard deviations above the mean would constitute a reasonable maximum for design, or:

$$\bar{V}_{\text{des max}} = 62 \text{ m sec}^{-1} = 210 \text{ ft sec}^{-1}$$

Excluding the yellow-dust devil from consideration, there are no conditions which can be visualized in which the latter wind speed would be encountered as a sharp-edged gust. If the shear (and eddy-generation) conditions typical of the thunderstorm are used as a basis of estimate (and this would be a very conservative basis since equivalent conditions would be rare on Mars) a value of about one-third of the design maximum speed would be indicated for the estimate of a design gust, or:

$$U_{\text{des}} = 21 \text{ m sec}^{-1} = 70 \text{ ft sec}^{-1}$$

Conclusions and Further Research:

Upon the basis of available observations and similarity to rotating fluid systems -- including Earth -- it has been possible to estimate a mean distribution of thermodynamic and wind variables for the lower Martian troposphere which appears to be consistent with present knowledge and which tests favorably in approximate radiation checks. From that distribution several magnitudes for preliminary design of exploratory entry vehicles for Mars are suggested.

In further research spatial and temporal variations from the means suggested, as well as improvement in estimate of their magnitudes, will be sought. In that approach, the global-modelling technique of Leovy and Mintz (Leovy and Mintz, 1966) probably has the greatest promise of confident and useful results as the programming relationships are subjected to further refinement (e. g. effects of clouds and scattering in radiation, additional heat sources and sinks in water vapor and carbon dioxide as working fluids, etc.).

There is a critical need for further sophisticated experiments and studies to determine the probable nature of the surface materials of Mars and threshold magnitudes of lifting of yellow-dust.

Additional studies, such as the excellent early work of Hess (Hess, 1950), which thoroughly assimilate the many excellent astronomical observations of Mars and relate pertinent features to the structure and circulation of the Martian atmosphere should be encouraged.

Repetitions and refinements of the occultation and spectrometric observations should yield either additional information or greater confidence in the observations already available.

The critical test of all prior estimates will, of course, be attained in the observations of the first probe to penetrate the Martian atmosphere. In a sense, this will be a conclusive test of the several concepts of atmospheric physics that have been brought to bear in estimating the structure and circulation of the Martian atmosphere, as well as of the many excellent observations that have produced essential basic data.

Acknowledgments:

The writer thanks the National Aeronautics and Space Administration and the McDonnell-Douglas Aircraft Corporation for their assistance in many of the studies underlying the results presented in this report. Humble gratitude is also due to the many competent scientists upon whose observations and theories the whole has been rested. To my research staff -- Mssrs. J. Vogel, W. Dannevik, Miss J. Orwig and Mrs. L. Marco and my able colleague, Prof. A. J. Pallmann -- many thanks.

REFERENCES

- Bates, F. C., 1966: The Martian Atmosphere: Thermodynamic Structure and Circulation; Consultant Report to McDonnell Aircraft Corporation.
- deVaucoulers, G., 1954: Physics of the Planet Mars; Faber and Faber Limited, London.
- Dollfuss, A., 1961: Visual Photographic Studies of Planets and Satellites; U. of Chicago Press, Chicago, Ill.
- Fultz, D., 1960: Experimental Models of Rotating Fluids and Possible Avenues for Further Research; Dynamics of Climate; Pergammon Press, New York.
- Goody, R. M., 1964: Atmospheric Radiation; Oxford at the Clarendon Press, London.
- Haurwitz, B., 1941: Dynamic Meteorology; McGraw-Hill Book Company, Inc., New York.
- Haurwitz, B., 1962: Thermally-driven Circulation; Beitr. Atm.; 35.
- Hess, S. L., 1950: Some Aspects of the Meteorology of Mars; Journal of Meteorology, 7, 1950.
- Johnson, F. S., 1965: Atmosphere of Mars; Science; 150.
- Kaplan, L. D., G. Munch and H. Spinrad, 1964: An Analysis of the Spectrum of Mars; J. Astroph.; 139.
- Kliore, A. et alia, 1965: Occultation Experiment: Results of the First Direct Measurement of Mars' Atmosphere and Ionosphere; Science; 149.
- Leovy, C. B. and Y. Mintz, 1966: A Numerical General Circulation Experiment for the Atmosphere of Mars; Memorandum RM-5110-NASA, Dec. 1966.
- Mintz, Y., 1961: The General Circulation of Planetary Atmospheres; The Atmosphere of Mars and Venus; Nat. Acad. of Sci., Nat. Res. Council, Publ., 944.
- Moroz, V. I., 1964: Infrared Spectrum of Mars; Astron. Zh., 41, 1964.
- Pallmann, A. J., 1966: Martian Atmosphere: Radiative Heating and Cooling Rate; Consultant Report to McDonnell Aircraft.
- Pettit, E., 1961: Planetary Temperature Measurements; Planets and Satellites; U. of Chicago Press, Chicago, Ill.
- Prabhakara, C. and J. S. Hogan, Jr., 1965: Ozone and Carbon Dioxide Heating in the Martian Atmosphere; J. Atm. Sci., 22.

REFERENCES cont'd.

Tang, W., 1965: Some Aspects of the Atmospheric Circulation on Mars;
NASA Contractor Report, NASA CR-262, NASA, Washington, D. C.

APPENDIX

The following is a computer program utilized to compute heating rates in ten 5-km. layers for any given fixed temperature distribution.

```

C PROGRAM MARS
C MARSRADCHEK USING 100PC CO2, NO SUSPENSIDS, NO SCATTERING PRESENT,
C LTE, DOPPLER BROADENING NEGLIGIBLE, NO SOLAR RADIATION FROM SURFACE
  REAL NET
  DOUBLE PRECISION DENS,CON1
  DIMENSION WNR(62),DELN(62),CON1(62),CON2(62),GAM(62),EOS(56),
1RFN(11,11),PM(23),TMP(11),DENS(62),FBU(11),FBD(11),BEE(11,6),
2EO(6),GA(6),BART(11,11,6),FLU(11),BURT(11,11,6),FLD(11),FRES
3(11),FNET(10),HEATV(10),HEAT(10),TRAT(10),BE(11,6),WN(6),DEL
4(6),CO1(6),CO2(6),TRANSD(11,11,6),TRANSU(11,11,6)
  READ(5,1)(WNR(I),DELN(I),CON1(I),CON2(I),GAM(I),EOS(I),I=1,56)
  READ(5,2)(WN(I),DEL(I),CO1(I),CO2(I),GA(I),EO(I),I=1,6)
1  FORMAT(2F6.1,F10.7,F5.2,F8.1,F7.3)
2  FORMAT(2F6.1,F10.7,F5.2,F8.1,F7.3)
100 READ(5,4)(PM(M),DENS(M),M=1,22)
4  FORMAT(F6.3,D11.9)
  READ(5,5)(TMP(M),M=1,11)
5  FORMAT(F5.0)
  READ(5,3)NTEST
3  FORMAT(I1)
  IF(NTEST)49,49,23
49 READ(5,50)PHI
50 FORMAT(F8.2)
  RPHI=PHI/57.2958
C EOS + EO SUBROUTINE
  DO 51 I=1,56
51 EOS(I)=SQRT(2.)*COS(RPHI)*EOS(I)
  DO 52 I=1,6
52 EO(I)=SQRT(2.)*COS(RPHI)*EO(I)
C RFN SUBROUTINE
23 DO 32 K=1,11
24 DO 31 M=1,11
  IF(K-M)27,26,25
25 P=K
  Q=M
  GO TO 28
26 RFN(K,M)=0.0
  GO TO 31
27 Q=K
  P=M
28 TSM=0.0
  IF(K-M)29,34,34
34 DO 35 I=M,K

```

APPENDIX cont'd.

```

    TSM=TSM+TMP(I)
35 CONTINUE
    GO TO 33
29 DO 30 I=K,M
    TSM=TSM+TMP(I)
30 CONTINUE
33 TBAR=TSM/(P-Q+1.0)
    SCH=189.2*TBAR/3.76
    HART=1.-EXP(-5000.*(P-Q)/SCH)
    IF(M-K)37,36,36
36 RFN(K,M)=(DENS(2*M)*SCH*HART)/0.001977
    GO TO 31
37 RFN(K,M)=(DENS(2*K)*SCH*HART)/0.001977
31 CONTINUE
32 CONTINUE
C FBD SUBROUTINE
    DO 7 K=1,11
    TMIN= 1./TMP(K)-0.00606
    BIT = 0.00207*PM(K+1)*RFN(K,1)
    SUM = 0.0
    DO 6 I=1,56
    NET=EOS(I)*DELN(I)*EXP(-SQRT(CON1(I)*(CON2(I)**2.)*EXP(TMIN)*BIT))
    SUM = SUM+ NET
    6 CONTINUE
    FBD(K)=0.636*SUM
    7 CONTINUE
C FBU SUBROUTINE
    DO 9 J=1,11
    K =12-J
    TMO=0.00431-1./TMP(K)
    BIT=0.00207*PM(K+11)*RFN(K,11)
    SUM=0.0
    DO 8 I=1,6
    BE(K,I)=0.000011925*(WN(I)**3)/(EXP(1.4398*WN(I)/TMP(K))-1.0)
    NET=BE(K,I)*DEL(I)*EXP(-SQRT(CO1(I)*(CO2(I)**2)*EXP(GA(I)*TMO)*BIT
1))
    SUM= SUM+ NET
    8 CONTINUE
    FBU(K)= 3.14159*SUM
    9 CONTINUE
C BEE AND TRANS SUBROUTINE
    DO 10 M=1,11
    DO 10 I=1,6
    BEE(M,I)=0.000011925*(WN(I)**3)/(EXP(1.4398*WN(I)/TMP(M))-1.0)
10 CONTINUE
    DO 41 K=1,11
    DO 41 I=1,6
    DO 41 M=1,11
    IF(M-K)40,40,41
40 TML=1./TMP(K)-1./TMP(M)

```

APPENDIX cont'd.

```

      BIT=0.00207*PM(K+M)*RFN(K,M)
      TRANSD(K,M,I)=EXP(-SQRT(CO1(I)*CO2(I)**2*EXP(GA(I)*TML)*BIT))
41  CONTINUE
      DO 43 J=1,11
      K=12-J
      DO 43 I=1,6
      DO 43 N=1,11
      M=12-N
      IF(M-K)43,42,42
42  TML=1./TMP(K)-1./TMP(M)
      BIT=0.00207*PM(K+M)*RFN(K,M)
      TRANSD(K,M,I)=EXP(-SQRT(CO1(I)*CO2(I)**2*EXP(GA(I)*TML)*BIT))
43  CONTINUE
C  FLD SUBROUTINE
      DO 11 K=2,11
      DO 11 I=1,6
      DO 11 M=1,10
      IF(M-K)44,11,11
44  BURT(K,M,I)=BEE(M,I)*(TRANSD(K,M+1,I)-TRANSD(K,M,I))
11  CONTINUE
      DO 14 K=2,11
      TOT= 0.0
      DO 13 I=1,6
      SUM = 0.0
      DO 12 M=1,10
      IF(M-K)45,12,12
45  SUM=SUM+BURT(K,M,I)
12  CONTINUE
      BLOT=DEL(I)*SUM
      TOT=TOT+BLOT
13  CONTINUE
      FLD(K)=3.14159*TOT
14  CONTINUE
C  FLU SUBROUTINE
      DO 15 J=2,11
      K=12-J
      DO 15 I=1,6
      DO 15 N=2,11
      M=12-N
      IF(M-K)15,46,46
46  BART(K,M,I)=BEE(M,I)*(TRANSD(K,M,I)-TRANSD(K,M+1,I))
15  CONTINUE
      DO 18 J=2,11
      K=12-J
      TOT=0.0
      DO 17 I=1,6
      SUM=0.0
      DO 16 N=2,11
      M=12-N
      IF(M-K)16,47,47

```

APPENDIX cont'd

```

47 SUM=SUM+BART(K,M,I)
16 CONTINUE
   BLAT=DEL(I)*SUM
   TOT=TOT+BLAT
17 CONTINUE
   FLU(K)=3.14159*TOT
18 CONTINUE
C FINAL SUBROUTINE
   FLD(1)=0.0
   FLU(11)=0.0
   FRES(1)=FBU(1)+FLU(1)-FBD(1)
   FRES(11)=FBU(11)-FBD(11)-FLD(11)
   DO 19 K=2,10
   FRES(K)=FBU(K)+FLU(K)-FBD(K)-FLD(K)
19 CONTINUE
   DO 20 L=1,10
   FNET(L)=FRES(L+1)-FRES(L)
   HEATV(L)=0.000002*FNET(L)
   HEAT(L)=HEATV(L)/DENS(2*L+1)
   TRAT(L)=HEAT(L)/7300000.0
20 CONTINUE
   WRITE(6,21) (FBD(K),FBU(K),FLU(K),FLD(K),FRES(K),K=1,11)
21 FORMAT(1H1,10X,3HFBD,13X,3HFBU,13X,3HFLU,13X,3HFLD,13X,4HFRES,/
11HO,5F16.4,/(1X,5F16.4))
   WRITE(6,22) (FNET(L),HEATV(L),TRAT(L),HEAT(L),L=1,10)
22 FORMAT(1HO,/1HO,10X,4HFNET,18X,5HHEATV,14X,4HTRAT,14X,4HHEAT,/
11HO,4F20.10,/(1X,4F20.10))
   WRITE(6,60) ((BEE(M,I),M=1,11),I=1,6)
60 FORMAT(1H1,10X,3HBEE,/1HO,6F11.7,/(1X,6F11.7))
   WRITE(6,61) (((TRANSD(K,M,I),K=1,11),M=1,11),I=1,6)
61 FORMAT(1H1,10X,6HTRANSD,/1HO,11F11.6,/(1X,11F11.6))
   WRITE(6,62) (((TRANSU(K,M,I),K=1,11),M=1,11),I=1,6)
62 FORMAT(1H1,10X,6HTRANSU,/1HO,11F11.6,/(1X,11F11.6))
   GO TO 100
   END

```

INPUT DATA

<u>I</u>	<u>WNR(I)</u> (cm ⁻¹)	<u>DELN(I)</u> (cm ⁻¹)	<u>CON1(I)</u> (atm/cm)	<u>CON2(I)</u> (atm ⁻¹)	<u>GAM(I)</u> (°K)	<u>EOS(I)</u> (ergs/cm ³ sec)
1	7750.	50.	.0005	.3	1.0	17.95
2	7700.	50.	.00012	.3	1.0	17.58
3	7650.	50.	.000015	.3	1.0	17.20
4	7600.	50.	.002	.3	1.0	16.86
5	7550.	50.	.00013	.3	1.0	16.71
6	7500.	50.	.0002	.3	1.0	16.35
7	7450.	50.	.00072	.3	1.0	16.12
8	7400.	50.	.000018	.3	1.0	15.88
9	7000.	50.	.00092	.3	1.0	13.40
10	6950.	50.	.002	.3	1.0	13.14
11	6900.	50.	.00012	.3	1.0	12.82
12	6550.	50.	.0000029	.3	1.0	10.93
13	6500.	50.	.00009	.3	1.0	10.71
14	6450.	50.	.0000029	.3	1.0	10.50
15	6400.	50.	.0000064	.3	1.0	10.29
16	6350.	50.	.0007	.3	1.0	10.02
17	6300.	50.	.000025	.3	1.0	9.77
18	6250.	50.	.00035	.3	1.0	9.52
19	6200.	50.	.00001	.3	1.0	9.35
20	6150.	50.	.00001	.3	1.0	9.05
21	6100.	50.	.000055	.3	1.0	8.83
22	6050.	50.	.000019	.3	1.0	8.61
23	5175.	50.	.0000039	.33	1.0	5.25
24	5125.	50.	.035	.33	1.0	5.09
25	5075.	50.	.03	.33	1.0	4.92

<u>I</u>	<u>WNR(I)</u>	<u>DELN(I)</u>	<u>CON1(I)</u>	<u>CON2(I)</u>	<u>GAM(I)</u>	<u>EOS(I)</u>
26	5025.	50.	.0075	.33	1.0	4.76
27	4975.	50.	.53	.33	1.0	4.60
28	4925.	50.	.02	.33	1.0	4.46
29	4875.	50.	.1	.33	1.0	4.32
30	4825.	50.	.06	.33	1.0	4.17
31	4775.	50.	.0013	.33	1.0	4.09
32	4725.	50.	.0003	.33	1.0	3.83
33	3825.	50.	.0001	.36	1.0	1.875
34	3775.	50.	.002	.36	1.0	1.805
35	3725.	50.	.27	.36	1.0	1.712
36	3675.	50.	5.0	.36	1.0	1.642
37	3625.	50.	17.0	.36	1.0	1.564
38	3575.	50.	6.0	.36	1.0	1.485
39	3525.	50.	.21	.36	1.0	1.413
40	3475.	50.	.005	.36	1.0	1.352
41	3438.	25.	.00002	.36	1.0	1.298
42	2460.	20.	.000022	.86	1.0	.388
43	2440.	20.	.00002	.86	1.0	.376
44	2420.	20.	.0005	.86	1.0	.363
45	2400.	20.	.0032	.86	1.0	.354
46	2380.	20.	1.6	.86	1.0	.345
47	2360.	20.	70.0	.86	1.0	.333
48	2325.	50.	20.0	.86	1.0	.316
49	2275.	50.	.7	.86	1.0	.289
50	2225.	50.	1006	.86	1.0	.264
51	2175.	50.	.00006	.86	1.0	.252

<u>I</u>	<u>WNR(I)</u>	<u>DELN(I)</u>	<u>CON1(I)</u>	<u>CON2(I)</u>	<u>GAM(I)</u>	<u>EOS(I)</u>
52	2125.	50.	.001	.86	1.0	.220
53	2075.	50.	.02	.35	1.0	.207
54	2025.	50.	.001	.35	1.0	.186
55	1975.	50.	.00005	.35	1.0	.177
56	1925.	50.	.002	.35	1.0	.160

<u>I</u>	<u>WN(I)</u>	<u>DEL(I)</u>	<u>CO1(I)</u>	<u>CO2(I)</u>	<u>GA(I)</u>	<u>EO(I)</u>
1	825.	50.	.000025	.24	3000.0	0.0
2	775.	50.	.002	.24	2000.0	0.0
3	725.	50.	.5	.24	1300.0	0.0
4	675.	50.	45.0	.24	400.0	0.0
5	625.	50.	2.5	.24	1000.0	0.0
6	575.	50.	.01	.24	20.0	0.0

Mean-Annual Subsolar-Meridian - 45° Latitude Sounding

<u>M</u>	<u>TMP (M)</u> (°K)	<u>M</u>	<u>PM (M)</u> (mb)	<u>DENS (M)</u> (g - cm ³)
1	165.0	1	0.0	0.000000064
2	163.0	2	0.02	0.000000097
3	162.0	3	0.03	0.000000130
4	160.0	4	0.04	0.000000163
5	159.0	5	0.05	0.000000229
6	157.0	6	0.07	0.000000328
7	155.0	7	0.10	0.000000430
8	175.0	8	0.13	0.000000598
9	195.0	9	0.18	0.000000798
10	215.0	10	0.24	0.00000110
11	233.0	11	0.33	0.00000155
		12	0.46	0.00000214
		13	0.63	0.00000295
		14	0.87	0.00000388
		15	1.21	0.00000490
		16	1.62	0.00000610
		17	2.14	0.00000753
		18	2.78	0.00000923
		19	3.58	0.00001110
		20	4.53	0.00001320
		21	5.60	0.00001580
		22	7.00	

Prabhakara and Hogan

<u>M</u>	<u>TMP (M)</u>	<u>M</u>	<u>PM(M)</u>	<u>DENS (M)</u>
1	160.0	1	0.0	0.0
2	164.0	2	0.03	0.000000099
3	168.0	3	0.04	0.000000120
4	174.0	4	0.05	0.000000141
5	180.0	5	0.07	0.000000212
6	185.0	6	0.10	0.000000316
7	190.0	7	0.15	0.000000445
8	195.0	8	0.19	0.000000576
9	200.0	9	0.26	0.000000754
10	210.0	10	0.33	0.000000965
11	230.0	11	0.43	0.00000122
		12	0.57	0.00000163
		13	0.74	0.00000206
		14	0.98	0.00000271
		15	1.28	0.00000354
		16	1.64	0.00000445
		17	2.13	0.00000571
		18	2.74	0.00000720
		19	3.52	0.00000911
		20	4.45	0.0000112
		21	5.56	0.0000133
		22	7.00	0.0000160

Johnson

<u>M</u>	<u>TMP (M)</u>	<u>M</u>	<u>PM(M)</u>	<u>DENS (M)</u>
1	115.0	1	0.0	0.0
2	117.5	2	0.004	0.000000004
3	120.0	3	0.006	0.000000017
4	122.5	4	0.009	0.000000037
5	125.0	5	0.013	0.000000050
6	130.0	6	0.017	0.000000075
7	135.0	7	0.03	0.000000184
8	140.0	8	0.04	0.000000321
9	160.0	9	0.07	0.000000356
10	185.0	10	0.10	0.000000422
11	210.0	11	0.15	0.000000607
		12	0.23	0.000000940
		13	0.39	0.00000147
		14	0.52	0.00000202
		15	0.79	0.00000309
		16	1.13	0.00000426
		17	1.68	0.00000588
		18	2.34	0.00000772
		19	3.21	0.00000970
		20	4.23	0.0000120
		21	5.46	0.0000145
		22	7.00	0.0000175

Gobdy

<u>M</u>	<u>TMP (M)</u>	<u>M</u>	<u>PM (M)</u>	<u>DENS (</u>
1	170.0	1	0.0	0.0
2	170.0	2	0.04	0.0000
3	170.0	3	0.06	0.0000
4	177.0	4	0.08	0.0000
5	185.0	5	0.11	0.0000
6	201.0	6	0.15	0.0000
7	217.0	7	0.21	0.0000
8	225.0	8	0.27	0.0000
9	233.0	9	0.37	0.0000
10	250.0	10	0.47	0.0000
11	270.0	11	0.61	0.0000
		12	0.78	0.0000
		13	0.99	0.0000
		14	1.26	0.0000
		15	1.59	0.0000
		16	1.98	0.0000
		17	2.46	0.0000
		18	3.07	0.0000
		19	3.85	0.0000
		20	4.78	0.0001
		21	5.72	0.0001
		22	7.00	0.0001

POSTMASTER: If Undeliverable (Section 158
Postal Manual) Do Not Return

"The aeronautical and space activities of the United States shall be conducted so as to contribute . . . to the expansion of human knowledge of phenomena in the atmosphere and space. The Administration shall provide for the widest practicable and appropriate dissemination of information concerning its activities and the results thereof."

—NATIONAL AERONAUTICS AND SPACE ACT OF 1958

NASA SCIENTIFIC AND TECHNICAL PUBLICATIONS

TECHNICAL REPORTS: Scientific and technical information considered important, complete, and a lasting contribution to existing knowledge.

TECHNICAL NOTES: Information less broad in scope but nevertheless of importance as a contribution to existing knowledge.

TECHNICAL MEMORANDUMS: Information receiving limited distribution because of preliminary data, security classification, or other reasons.

CONTRACTOR REPORTS: Scientific and technical information generated under a NASA contract or grant and considered an important contribution to existing knowledge.

TECHNICAL TRANSLATIONS: Information published in a foreign language considered to merit NASA distribution in English.

SPECIAL PUBLICATIONS: Information derived from or of value to NASA activities. Publications include conference proceedings, monographs, data compilations, handbooks, sourcebooks, and special bibliographies.

TECHNOLOGY UTILIZATION PUBLICATIONS: Information on technology used by NASA that may be of particular interest in commercial and other non-aerospace applications. Publications include Tech Briefs, Technology Utilization Reports and Notes, and Technology Surveys.

Details on the availability of these publications may be obtained from:

SCIENTIFIC AND TECHNICAL INFORMATION DIVISION

NATIONAL AERONAUTICS AND SPACE ADMINISTRATION

Washington, D.C. 20546